International Journal of GEOMATE, Feb., 2020, Vol.18, Issue 66, pp. 1 - 8
ISSN: 2186-2982 (P), 2186-2990 (O), Japan, DOI: https://doi.org/10.21660/2020.66.9150
Geotechnique, Construction Materials and Environment

TIME-DEPENDENT BEHAVIOUR OF PILED RAFT FOUNDATIONS ON SATURATED CLAY: EXPERIMENTAL INVESTIGATIONS

*Lua Hoang[1,2] and Tatsunori Matsumoto[1]

[1]Faculty of Geosciences and Civil Engineering, Kanazawa University, Japan; [2]Thuyloi University, Vietnam

*Corresponding Author, Received: 10 June 2019, Revised:01 Dec. 2019, Accepted: 01 Jan. 2020

ABSTRACT: When designing a piled raft foundation (PR) on clay, it is necessary to understand the time-dependent behaviour of the foundation because stresses and strains in clayey ground will change for a long time after the construction, due to consolidation processes of the ground. This paper, therefore, aims to investigate the long-term behaviour of PRs through small-scale physical modelling. In the experiments, the model ground was prepared by consolidating a slurry mixture of Kasaoka clay and silica sand. The model foundations consisted of a square raft having a width of 125 mm and 4 or 9 piles having a length of 150 mm. For the loading test of PR, vertical load was increased by multiple steps and each load step was maintained to observe the long-term behaviour. The experimental results show that the piles effectively suppress the foundation settlement for relatively smaller loads. In the primary consolidation stage, the pile resistance increases with elapsed time while the raft resistance decreases. This is caused by the dissipation of pore water pressure and the corresponding increase of effective stresses of soils below the raft base. In the secondary consolidation stage, for the case of 4-pile PR, the resistances of both the raft and piles are stable although creep settlement continues. For the secondary consolidation stage of 9-pile PR, pile load reduces slightly under smaller applied loads and stable under larger applied loads. In general, the 9-pile PR reduces the foundation settlement significantly under smaller applied loads, compared to the 4-pile PR.

Keywords: Piled raft, Clayey ground, Experiment, Consolidation, Pile number

1. INTRODUCTION

In recent years, there has been an increasing need to construct heavy structures, especially in urban areas. To support these structures, piled raft (PR) is a favourable foundation type because of its cost-effectiveness and safety, as both raft and piles share the load together.

The behaviour of PRs in clay have been investigated in many researches. In most of these researches, numerical methods were used to solve the behaviour. Physical modelling of PRs on clay subjected to vertical loads were carried out in a few researches. In these experimental studies, one of the main targets is investigating how to arrange pile effectively to control the load-settlement relationship or to minimize total settlement and differential settlement of the foundation. Another one is studying the load sharing between the raft and the piles in the PR foundation. Cooke [1] carried out a series of model tests on unpiled rafts, free-standing piles and piled rafts of various sizes on homogeneous stiff clay, and pointed out that, when the ratio of pile length to raft breadth was less than 2, the settlement reduction may be between 1/3 and 1/2 of the unpiled raft settlement under the same applied load. He suggested that to obtain the maximum benefit from piles included for reducing settlement, the piles should be long relative to the breadth of the foundaiton. Horikoshi and Randolph [2] used centrifuge modelling to investigate behaviour of piled raft foundations with different pile numbers, and found out that a small centred pile group could reduce the differential settlement of a PR effectively. Recently, other experiments were conducted to investigate more detailed on how the pile number, pile size, pile spacing and raft size affect the settlement and the load sharing of PRs on clay [3–9]. From the literature review, most of the experiments aimed to investigate the immediate behaviour of PRs until the full construction load, disregarding long-term behaviour after full construction load was achieved. However, if a PR is located on saturated clayey ground, the foundation will continue to settle for a very long time after the construction, due to the dissipation of excess pore water pressure in the primary consolidation stage and creep behaviour of the ground in the secondary consolidation stage.

Hence, one of the main purposes of this research is to study the time-dependent behaviour of PRs on saturated clay through small-scale physical modelling. Focuses are placed on the settlement of the foundation, and on the change of load sharing by the raft and piles with time. Load tests on two PRs with different pile numbers were carried out to investigate the effect of pile number on load distribution and on the foundation settlement.

2. EXPERIMENT DESCRIPTION

2.1 Model Ground

2.1.1 Preparation of the model grounds

Clay ground was prepared in a cylindrical chamber of height 420 mm and diameter 420 mm. The soil used for the model ground was a mixture of Kasaoka clay powder and silica sand #6.

The model ground was prepared as follows: Firstly, Silica sand #3 was poured into the chamber, and compacted in saturated condition until it reached a high relative density D_r of 81% and a thickness of 50 mm for a bottom drainage layer. This drainage layer was considered as a stiff layer. Secondly, in a rectangular basin, Kasaoka clay powder and Silica sand #6 were mixed at a dry mass ratio of 1:1 (K50S50). Water was then added to the mixed soil to have a soil slurry with a water content of 1.3 times the liquid limit *LL*. This soil slurry was poured into the chamber to have an initial thickness of 370 mm. The soil was then left to consolidate under its self-weight for two days. After that, a surface layer of silica sand #6 of thickness 10 mm was placed on the clay to provide the top drainage layer, and a rigid circular loading plate was placed on the top. Next, vertical load on the loading plate was increased to consolidate the soil one-dimensionally in several steps, up to a vertical stress of 100 kPa. Each load step was maintained until the degree of consolidation reached 90% following the one-dimensional consolidation theory of Terzaghi. The final load step was kept for an additional week to have higher degrees of consolidation. Finally, the consolidation pressure was removed and the ground was allowed for the swelling process in 10 days.

2.1.2 Soil property investigation

T-bar tests, cone penetration tests (CPTs) and unconfined compression tests (UCTs) were carried out immediately after completion of the load test of each model foundation. In each model ground, two T-bar tests (T1 and T2) were conducted at the locations far from the load test area in order to estimate the undrained shear strength of the original model ground without the effect of the loading test of PR. Three other T-bar tests (T3, T4, and T5) were carried out at the locations beneath the raft base (loading area) in order to obtain the effect of the load test of PR on the ground strength. Three CPTs were also conducted in one experiment. Figure 1(a) shows the locations of the T-bar tests and the CPTs in the two experiments. Undrained shear strength c_u was deduced from the average stress acting on T-bar cylinder $q_{u\,T\text{-}bar}$ using an empirical equation [10] (see Eq. (1)) or from the cone tip resistance $q_{u\,kt}$ using an empirical equations [10] (see Eq. (2)):

$$c_u = q_{T\text{-}bar} / N_{T\text{-}bar} = P / (d_{T\text{-}bar} L_{T\text{-}bar} N_{T\text{-}bar}) \quad (1)$$

where $N_{T\text{-}bar}$ is the resistance factor for the T-bar and was taken as 10.5 [10].

$$c_u = (q_{u\,kt} - \sigma_{vo}) / N_{kt} \quad (2)$$

where σ_{vo} is the total overburden stress and N_{kt} is the cone resistance factor, taken as 12 [10].

As for UCTs, soil specimens were sampled from different depths of each ground. Locations of the specimens were also selected at, near and far from the loading area (Fig. 1(a)). c_u was estimated from unconfined compression strength q_u as $c_u = q_u /2$.

Figure 1(b) shows the distributions of c_u of the model grounds with depth obtained from the three different methods. The c_u varied with depth, and similar results were obtained for both the model grounds. c_u of the original model ground could be expressed approximately by the following equation:

$$c_u \text{ (kPa)} = 9 \text{ (kPa)} + z \text{ (mm)} \times 0.04 \text{ (kPa/mm)} \quad (3)$$

To obtain other properties of the model grounds, laboratory soil tests such as oedometer, Atterberg limits, the density of soil particle, saturated density, and water content tests were conducted, and the results are summarised in Table 1.

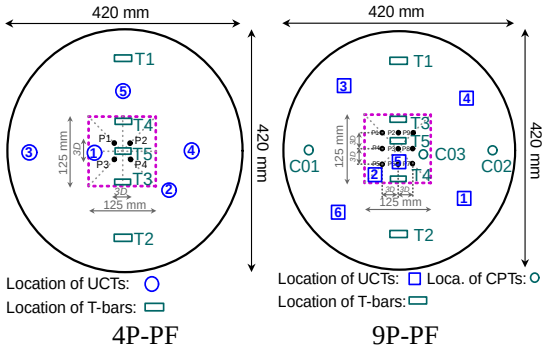

(a) Location of T-bar tests, CPTs and UCTs

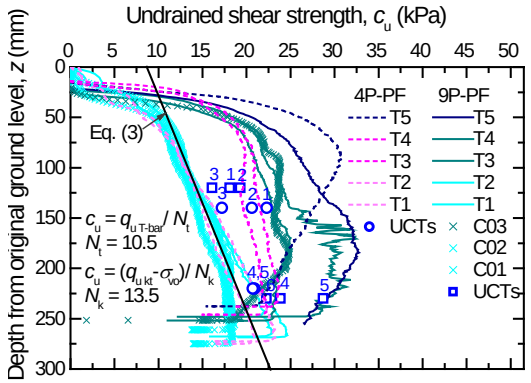

(b) Profile of undrained shear strength with depth

Fig. 1 Distribution of c_u with depth

Table 1 Properties of the model ground soil

Parameter	Notation and unit	Value
Density of soil particle	ρ_s (Mg/m^3)	2.653
Saturated density	ρ_{sat} (Mg /m^3)	1.98
Liquid limit	LL (%)	33.9
Plastic limit	PL (%)	13.6
Compression index	C_c	0.291
Swelling index	C_s	0.055
Water content*	w (%)	26.2
Void ratio*	e	0.7

Note: * after consolidating with vertical pressure of 100 kPa

2.2 Model Foundations

Model piles used in this study were ABS (Acrylonitrile Butadiene Styrene) solid bars (Fig. 2(a)) having a diameter D of 10 mm and a length L of 150 mm. Young's modulus E_p and Poisson's ratio ν of the model piles are 2920 N/mm^2 and 0.406, respectively. In order to measure axial forces along each pile, strain gauges (SGs) were attached on the pile shaft at 4 different levels as shown in Fig. 2(a). Cross gauges were used at all locations to eliminate the effect of temperature on the experimental results. The model raft was a square aluminium plate with a thickness of 12 mm and a width of 125 mm (Fig. 2(b)). The raft could be regarded as rigid.

In the experiments, the foundation models included an unpiled raft (UR), a single pile (SP), a 4-pile pile foundation (4P-PF), and a 9-pile pile foundation (9P-PF).

Figures 2(c) and (d) show the dimensions of the pile foundation models. Both the pile foundations (PFs) had the same centre-to-centre pile spacing s = 3D.

2.3 Test Procedure

Figure 3 shows the set-up of an experiment. The loading system in the experiment included an air cylinder to apply constant vertical load, a load cell to measure the applied load and 4 dial gauges to measure settlements of the foundation. One pore water pressure transducer and one earth pressure cell were installed at the locations near the raft base centre.

Prior to the load test of PFs, vertical static load tests on a single pile (SP) and an unpiled raft (UR) were carried out to obtain the bearing capacity of each element and to determine the magnitude of the vertical load to be applied on the piled rafts.

As for the load tests of the pile foundations, the piles were firstly jacked into the ground one by one with a centre-to-centre pile spacing s = 3D. Thereafter the raft was placed on the pile heads with a gap of around 5 mm between the raft base and the ground surface, and vertical static loading of the pile group (PG) was conducted in a displacement-controlled manner. The PG changed to piled raft (PR) after the raft base touched the ground surface. In the piled raft condition, vertical load was increased by 4 steps on 4P-PF and 5 steps on 9P-PF in a load-controlled manner. Each load step was maintained for a reasonable time to obtain the long-term behaviour of the foundation.

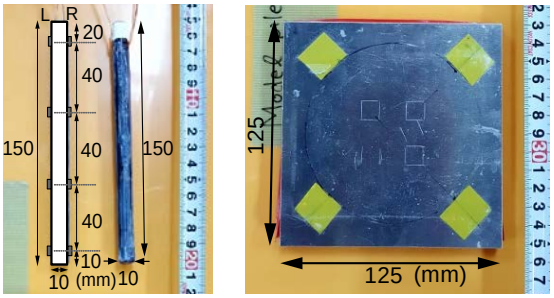

(a) Model piles and locations of SGs (b) Model raft

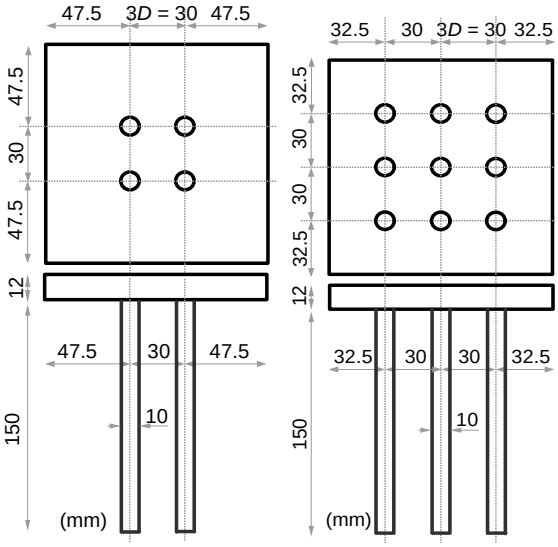

(c) 4P-PF (d) 9P-PF

Fig. 2 Model piles, raft and pile foundations

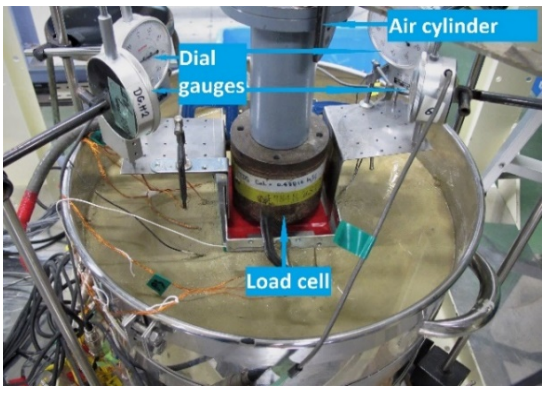

Fig. 3 The set-up of an experiment

3. EXPERIMENTAL RESULTS

3.1 Bearing Capacity of Single Pile and Unpiled Raft

Figure 4 shows the results of vertical load tests of the single pile (SP) and the unpiled raft (UR). The bearing capacity of UR and SP were about 2100 N and 100 N, respectively. The sum of bearing capacity of UR and 4 times of an SP or 9 times of an SP was 2500 N or 3000 N, respectively. Based on these results, the loads applied on the 4P-PF were determined to be 750, 1250, 2000 and 2500 N respectively, corresponding to 30% (Factor of safety F_S = 3.3), 50% (F_S = 2), 80% (F_S = 1.25) and 100% (F_S = 1.0) of the predicted total bearing capacity. For 9P-PF, the same 4 load steps were applied in order to compare with 4P-PF. One more final load step, P = 3000 N, corresponding to 100% of the predicted capacity of 9P-PF was applied.

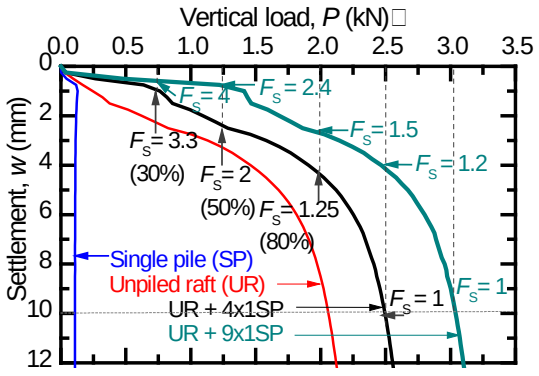

Fig. 4 Load settlement relations of SP and UR

3.2 Settlement and Pile Respond in PR Condition

3.2.1 Immediate behaviour - load-increasing stage

Figure 5(a) shows the relationships between the applied load P and the settlement w with the elapsed time t of the 4P-PF. Figures 5(b), (c), (d) and (e) are zoom-ins of the load-increasing stages of the 1st, 2nd, 3rd and 4th load steps of 4P-PF, respectively. The change of load carried by the piles is also shown in Fig. 5. Figure 6(a) shows the changes of excess pore water pressure (PWP) and settlement with time for the whole experimental duration of the 4P-PF. Figures 6(b), (c), (d) and (e) are zoom-ins of the load-increasing stages of the 1st, 2nd, 3rd and 4th load steps of 4P-PF, respectively.

Figures 7 and 8 show the corresponding results of 9P-PF.

Let us focus first on the results of the 4P-PF. It should be noted that the bearing capacity of a single pile was around 100 N. The applied load, P = 750 N, of the 1st load step was less than 9 times of the bearing capacity of an SP, but almost a double of 4 times of the bearing capacity of an SP.

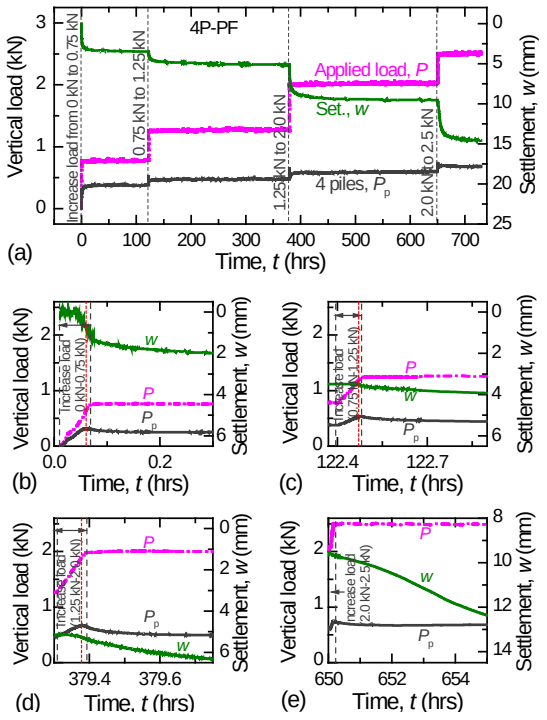

Fig. 5 Changes with time of load and settlement of 4P-PF: (a) full-time of loading test; (b), (c), (d) and (e) zoom-in the load-increasing stage of 1st, 2nd, 3rd, and 4th load step, respectively

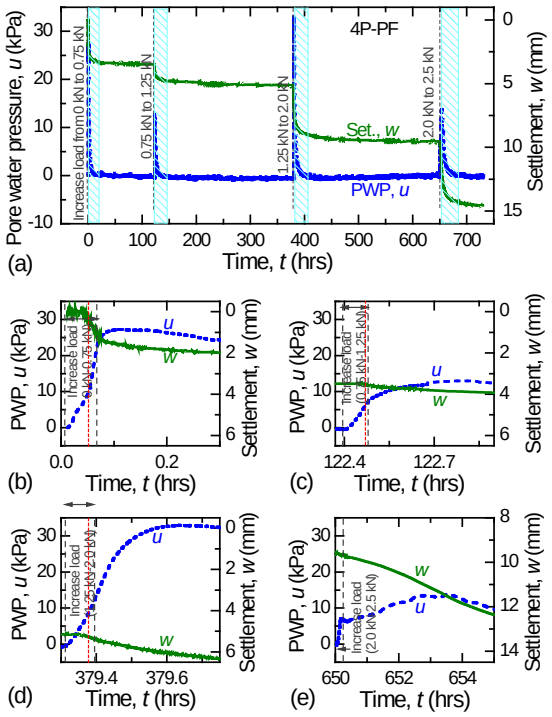

Fig. 6 Changes with time of PWP and settlement of 4P-PF: (a) full-time of loading test; (b), (c), (d) and (e) zoom-in the load-increasing stage of 1st, 2nd, 3rd, and 4th load step, respectively

Figure 5(b) shows that, at the early period of the load-increasing stage, the increase of the settlement was minor. The reason for this phenomenon is that, when the initial small loads were applied, the resistance of piles increased rapidly to support the load, and the increase of pile resistance was almost equal to the increase of the applied load.

Hence, the piles were effective at suppressing the settlement of the foundation in this early duration. The foundation then started settling while the pile resistance increased to a temporary peak in this load step. After the pile resistance reached the peak, the settlement of the foundation increased rapidly, and the pile resistance reduced. The raft load P_r is obtained as the difference between the applied load P and the pile load P_p.

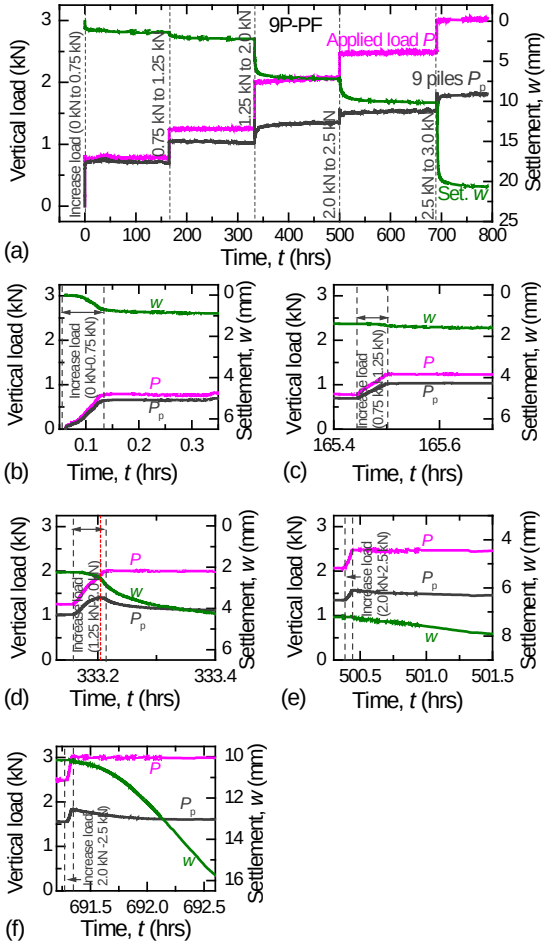

Fig. 7 Changes with time of load and settlement of 9P-PF: (a) full-time of loading test; (b), (c), (d) and (e) zoom-in load- increasing stages of 1st, 2nd, 3rd and 4th load step, respectively

Let us look at Fig. 6(b). It is clearly seen that PWP started increasing with the increasing settlement, and PWP increased sharply after the pile resistance reached the peak. The results show that after the applied load reached its target value and remained unchanged at P = 0.75 kN, the PWP continued to increase in short duration to reach a peak. In this paper, the load-increasing stage refers to the time from the start of increasing the applied load to the time of the peak PWP. Soon after the PWP reached the peak, the pile resistance decreased to the lowest value in this load step. Similar trends were measured for the other load steps (Figs. 5(c), (d), (e) and Figs. 6(c), (d), (e)), however, in the other load steps, both the raft and pile resistance increased from the start of load-increasing stage to support the applied load.

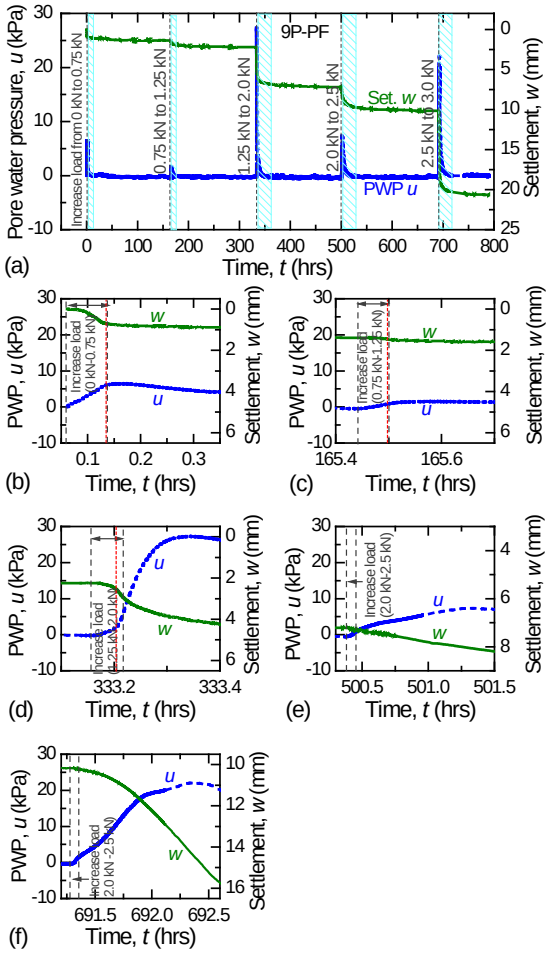

Fig. 8 Changes with time of PWP and settlement of 9P-PF: (a) full-time of loading test; (b), (c), (d) and (e) zoom-in load- increasing stages of 1st, 2nd, 3rd and 4th load step, respectively

Let us turn to the behaviour of 9P-PF. Comparing the results of 9P-PF with the results of 4P-PF, in the 1st and 2nd load steps (see Fig. 7(b) and Fig. 7(c), respectively), the settlements of 9P-PF were much smaller (about a half of the corresponding settlement of 4P-PF) and the reduction of pile resistance after reaching the peak did not occur. Figures 8(b) and 8(c) also indicate that the increments of PWP beneath the raft base of

9P-PF were quite small in these steps. The reason for the differences is that the 9P-PF had a larger number of piles, and the applied loads *P* in the first two load steps are not large, in comparison with the bearing capacity of the 9 piles. Therefore the applied loads were mainly carried by the piles in these load steps.

In the 3rd, 4th and 5th load steps where *P* was sufficiently large, compared with the bearing capacity of 9 times of an SP, the results of the 9P-PF have similar trends to the results of 4P-PF (i.e., the pile resistance increased to a temporary peak and then decreased; the PWP increased sharply with time after the peak pile resistance and reached a peak in a short duration after the applied load reached its target value).

It is interesting to notice that in both the foundations, the peak pile resistances increased with increasing the applied load. For example, the peak pile resistance in the 4 load steps, P = 0.75, 1.25, 2.0 and 2.5 kN, were 0.32, 0.53, 0.68 and 0.75 kN for 4P-PF, and 0.66, 1.02, 1.42 and 1.57 kN for 9P-PF, respectively. For 9P-PF, when the applied load increased to 3 kN, the resistance of the 9 piles reached a peak of 1.85 kN (average 205 N per pile) which was a double of 9 times the resistance of a single pile (around 100 N per pile). The increase of the pile resistance with increasing the applied load is caused by the increase of effective stresses in the ground, which will be explained in the next section.

3.2.2 Long-term behaviour - primary consolidation stage

The PWP dissipated after the load-increasing stage and returned to almost zero. These time durations could be regarded as primary consolidation stages (highlighted areas on Figs. 6(a) and 8(a)). These figures show that the settlement rates in the primary consolidation stages were roughly proportional to the dissipation rates of the PWP, and notable parts of settlements occurred in these stages.

The changes in raft load, pile load, and PWP with time of 4P-PF and 9P-PF are shown in Fig. 9(a) and Fig. 10(a), respectively. Figure 9(b) is the zoom-in of the primary consolidation stage of the 1st load step of 4P-PF and Figs. 10(b) and (c) are the zoom-ins of the primary consolidation stage of the 1st and the 3rd load steps of 9P-PF, respectively. Figures 9(b), 10(b) and 10(c) show clearly that, during the primary consolidation stages, the loads supported by the raft decreased while the loads supported by the piles increased with the elapsed time. In the 1st load step of 9P-PF (Fig. 10(b)), the peak PWP (7.5 kPa) was small and the increment of pile load was also small (0.055 kN). In the 3rd load step (Fig. 10 (c)), the peak PWP (30.3 kPa) was larger and the increment of pile load was also larger (0.19 kN). The magnitude of the increment of pile

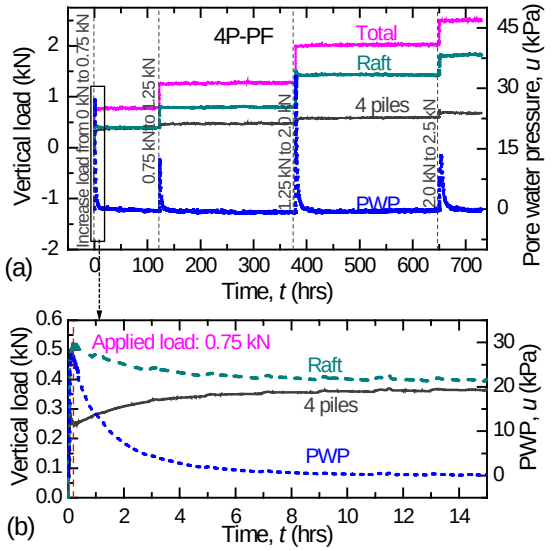

Fig. 9 Load transfer with time of 4P-PR: (a) full-time; (b) zoom-in of the first loading step

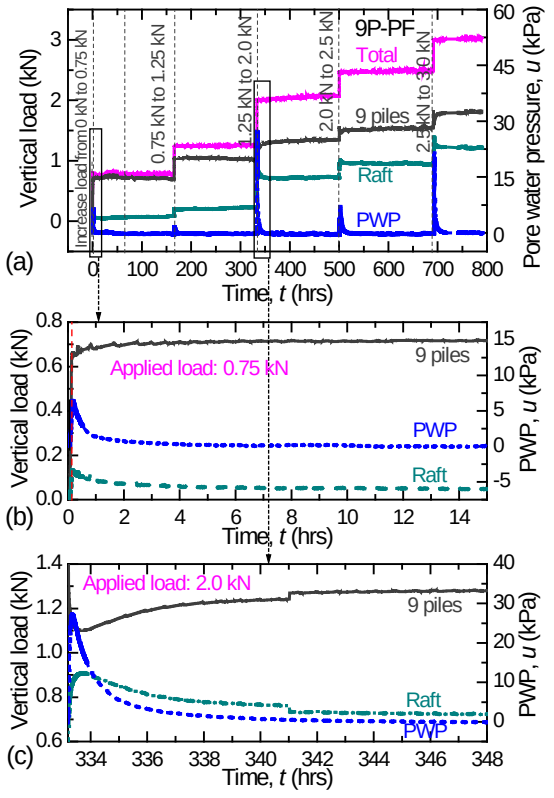

Fig. 10 Load transfer with time of 9P-PR: (a) full-time; (b) and (c) zoom-ins of the primary consolidation stage the 1st and 3rd load steps, respectively

resistance during the primary consolidation stage was roughly proportional to the magnitude of the increment of PWP during the load-increasing stage.

Hence, this phenomenon is caused by the consolidation process of the ground. The dissipation of the PWP causes the corresponding increase of the effective stress in the ground, resulting in the

increase of pile resistances. The effective stresses in the soil just beneath the raft increased also. However, as the raft load included the PWP, the raft load decreased because of the PWP dissipation. Similar trends were measured in the other load steps.

Let us look back at Fig. 1(b), in which c_u of the model grounds with and without the effect of the load tests of PRs were presented. It is clearly seen from the figure that, after the load test of PRs, within a depth of 190 mm from the raft base ($\simeq$ 1.5 times of the raft width), c_u was higher at the raft edge areas (T3, T4 and C03) and was highest at the centre area of the raft base (T5), in comparison with the original state (T1 and T2, C01 and C02). Furthermore, c_u beneath the raft base centre was much greater than c_u of the original ground within a depth of 75 mm for the 4P-PF, and of 150 mm for the 9P-PF. For deeper depths, the difference of c_u between the loading area and the original area became smaller with increasing depth. The results indicate that the area affected by the loading of 9P-PF was deeper than that of 4P-PF. The results of UCTs also presented similar trends. Therefore, it is clear that the consolidation process increased ground strength and stiffness.

3.2.3 *Long-term behaviour - secondary consolidation stage*

After the primary consolidation stages, the foundation continued to settle due to the creep phenomenon of the ground. This phenomenon was seen clearly in Fig. 6(a) for 4P-PF and Fig. 8(a) for 9P-PF. Here let us define the creep settlement index C_{cs} as follows where B is the raft breadth:

$$C_{cs} = \mathrm{d}(w/B)/\mathrm{d}(\log t) \quad (4)$$

In 4P-PF, C_{cs} for the 4 load steps of P = 0.75, 1.25, 2.0 and 2.5 kN were 0.00057, 0.0014, 0.0017 and 0.0165, respectively. The corresponding values for 9P-PF were 0.0005, 0.0021, 0.0118 and 0.0083. For the applied load of 3.0 kN, C_{cs} of 9P-PF was 0.0162. Basically, C_{cs} became larger as larger load was applied.

3.3 Load Distribution in Piled Raft Foundations

Figure 11 shows the proportions of loads shared by the raft and the piles with elapsed time in cases of (a) 4P-PF and (b) 9P-PF.

During the load-increasing stages: At the early duration of load-increasing stage of the 1st load step, the load was mainly carried by the piles until the piles reached their peak resistance, as mentioned above. In the other load steps, both the pile and raft resistances increased to support the load from the start of the load-increasing stage. After the peak pile resistance, the increment of the applied load was temporarily carried by the raft, therefore the proportion of the raft load increased quickly at the end of the load-increasing stages. Note again that the proportion of raft load in load-increasing stage includes the uplift force due to PWP.

During the primary consolidation stages: In both the foundations, the proportion of the load supported by the raft decreased in the primary consolidation stages meanwhile the proportion of the load carried by the piles increased with the elapsed time. This is due to the dissipation of the PWP at the raft base as described in the previous section.

During the secondary consolidation stages: For the case of 4P-PF, the proportions of loads shared by the raft and the piles were stable with time in all the 4 load steps, although the creep settlement of the foundation continued. For the case of 9P-PF, the proportion of the load supported by the raft increased slightly in the 1st and 2nd load steps, in which the applied load was mainly carried by the piles (above 80%). In the 3rd, 4th and final load steps, the proportion of loads carried by the raft and the piles were stable with time. This trend of load sharing of 9P-PF became similar to the trend of 4P-PF.

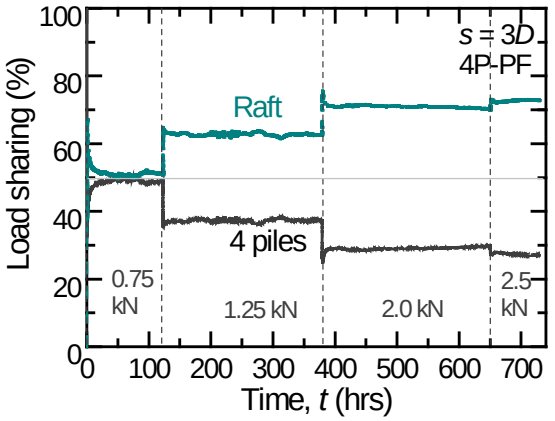

(a) 4P-PF

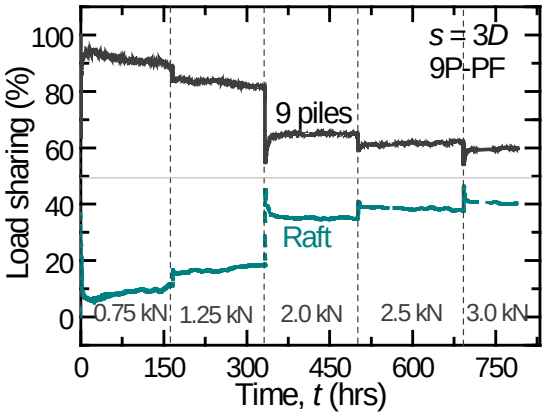

(b) 9P-PF

Fig. 11 Load sharing ratio with time in the PRs

In general, the proportion of the load supported

by the raft increased with increasing the applied load, and the raft carried notable parts of the applied load at relative larger loads. On the other hand, the piles also supported the applied load effectively. For 4P-PF, although only 4 piles were used, the piles carried about 50% of the applied load in the 1st load step and 30% of the applied load in the last load step. For 9P-PF, the 9 piles carried the major parts of the applied load in the first two load steps and carried about 60% of the total load at the final load step.

It is interesting that, at the end of the final load steps, the measured results show that the average load supported by each pile in both the piled raft foundations (175 N for 4P-PF case and 205 N for 9P-PF case) are much higher than the bearing capacity of a single pile (100 N).

4. CONCLUDING REMARKS

In this paper, long-term behaviours of PR models on saturated clay was investigated through small-scale physical modelling.

Main findings from this study are as follows:

(1) Piles were effective at supporting the load and suppressing the settlement of the foundation for relatively small applied loads. When the applied load was large enough, in comparison with the pile resistance, the increment of the applied load was mainly carried by the raft.
(2) Stresses from the raft base cause consolidation of the ground. Consequently, the effective stresses in the ground and ground stiffness increase, resulting in the increase of the pile resistance.
(3) After the primary consolidation stages, the creep settlement continued. For 4P-PF case, the loads supported by both the raft and the piles were stable with time (with creep settlement). For 9P-PF case, the pile load was slightly reduced under smaller applied loads, and stable under larger applied loads.
(4) The 9P-PF reduces the foundation settlement significantly under small applied loads, compared to the 4P-PF.

5. ACKNOWLEDGEMENTS

The authors gratefully acknowledge the excellent technical support of Mr Shimono Shinya, a technician of the Department of Environmental Design, Kanazawa University. The authors thank Mr Dao Xuan Khang, a master student of Geotechnical Engineering laboratory, Kanazawa University for his valuable help in experimental work.

6. REFERENCES

[1] Cooke R.W., Piled Raft Foundations on Stiff Clays - A Contribution to Design Philosophy. Geotechnique, Vol.36, Issue 2, 1986, pp.169–203.
[2] Horikoshi K. and Randolph M.F., Centrifuge Modelling of Piled Raft Foundations on Clay. Geotechnique, Vol.46, Issue 4, 1996, pp.741–752.
[3] Bajad S.P. and Sahu R.B., Optimum Design of Piled Raft in Soft Clay – A Model Study, in Proc. Indian Geotechnical Conference IGC–2009, pp.131–134.
[4] Horikoshi K., Optimum Design of Piled Raft Foundations. PhD thesis, The University of Western Australia, Perth, 1995, pp.1–330.
[5] Mandal S. and Sengupta, S., Experimental Investigation of Eccentrically Loaded Piled Raft Resting on Soft Cohesive Soil. Indian Geotech. J., Vol. 47, Issue 3, 2017, pp.314–325.
[6] Rodriguez E., Cunha R.P. and Caicedo B., Conference proceedings, in Proc. 9th Int. Conf. on Physical Modelling in Geotechnics, Vol.2, Issue 21, 2018, pp.1407–1412.
[7] Roy S., Chattopadhyay B.C. and Sahu R.B., Conference proceedings, in Proc. Indian Geotechnical Conference, 2011, pp.879–882.
[8] Thoidingjam D., Prasad D.S.V. and Devi D.K.R., Effect of Number of Pile in Pile-Raft System in Organic Clay. IOSR J. Mech. Civ. Eng., Vol. 13, Issue 4, 2016, pp.83–88.
[9] Thoidingjam D. and Devi K.R., Behavior of Pile Raft Foundation in Organic Clay. Indian J. Sci. Technol., Vol. 10, Issue 31, 2017, pp.1–4.
[10] Low H.E., Lunne T., Andersen K.H., Sjursen M.A., Li X. and Randolph, M.F., Estimation of Intact and Remoulded Undrained Shear Strengths from Penetration Tests in Soft Clays. Geotechnique, Vol.60, Issue 11, 2010, pp.843–859.